

Curvature and Solidification*

ALEXANDRE JOEL CHORIN

*Department of Mathematics and Lawrence Berkeley Laboratory,
University of California, Berkeley, California 94720*

Received February 7, 1984

A method is presented for finding the osculating circle, and thus the curvature and the normal, of a curve defined by an array of partial volumes. This method is applied, within the framework of an enthalpy formulation, to the solutions of model equations that describe the motion of a front separating ice and supercooled water. For short to moderate times the numerical results agree well with available theory; at longer times a morphological oscillation is observed. Such an oscillation was seen in earlier calculations but is not predicted by linearized stability theory. Some speculations regarding its origin are offered. © 1985 Academic Press, Inc.

INTRODUCTION

There are a number of problems in which it is necessary to evaluate the curvature or to find the normal of a computed surface, for example, in combustion theory (see, e.g., Markstein [10] and Sethian [16, 18]), in the theory of water waves (Stoker [21]), and more generally in flows with a free surface (Nichols *et al.* [12]), and in problems involving solidification and the growth of dendrites (see, e.g., Langer [7]). Numerical methods for evaluating curvature are presented, e.g., in Nichols *et al.* [12] and Smith [20], where some of the difficulties are noted. In the present paper we present an iterative algorithm for finding the osculating circle, and thus the curvature and also the normal, of a curve defined by an array of partial volumes. The method generalizes easily to the evaluation of the mean curvature of a surface in three dimensions. Partial volumes have emerged as a natural and effective way for describing moving boundaries, see, e.g., Noh and Woodward [13], Chorin [2], Ghoniem *et al.* [5], Hirt and Nichols [6] and Sethian [16, 17]. If the partial volumes are given accurately, the algorithm is accurate and reliable, albeit not necessarily inexpensive.

We apply our algorithm to the solution of a set of equations that has arisen in the analysis of solidification in a supercooled environment (the kind of situation where morphological instability and dendrite formation can occur). The boundary

* Work partially supported by the Director, Office of Energy Research, Office of Basic Energy Sciences, Engineering and Geosciences Division of the U.S. Department of Energy, under Contract DE-AC03-76SF00098.

conditions at the solid's boundary, derived from the Gibbs-Thomson relation, involve the boundary's curvature (see, e.g., Turnbull [22], Sekerka [15], Langer [7], and Smith [20]). The method of solution relies on a weak "enthalpy" formulation, previously studied for simpler problems by Rogers *et al.* [14], Shamsundar and Sparrow [19], Brezis and Crandall [1], and Majda [8]. The enthalpy formulation has already been adapted to the present problem, along different lines, by Smith [20].

Smith observed a discrepancy between his numerical results and the predictions of a linearized stability theory after perturbations grow to finite but small size; we had expected that a more accurate curvature evaluation and other improvement in the method would remove that discrepancy. This has not proved to be the case, and, as far as can be judged from [20], our results are comparable with Smith's. Some speculation is offered about the reason for the discrepancy; one possibility is that linearized theory does not faithfully describe the instability in the presence of finite amplitude perturbations. Doubts are also cast on the well-posedness of the initial value problem for the model equations, and on their usefulness as a description of the physics of solidification.

OSCULATING CIRCLES AND THE CURVATURE OF A CURVE DEFINED BY PARTIAL VOLUMES

Consider a plane region D covered by a square grid of mesh width h . In D lies a curve Γ dividing D into several disjoint pieces. Assume for the sake of simplicity that there are only two pieces; the discussion extends trivially to the more general case. Imagine that one of the regions is black and the other white, and agree that the curvature is positive at a point of Γ if the center of the osculating circle at that point is on the black side of the curve.

In each mesh cell, of center (ih, jh) , i, j integers, we are given a number $f_{i,j}$, $0 \leq f_{i,j} \leq 1$; $f_{i,j}$ is the black fraction of the area of the cell. The $f_{i,j}$ are known as "partial volumes." It is assumed in this section that the $f_{i,j}$ corresponding to Γ are known accurately. If they have been determined by integration it is assumed that appropriate precautions have been taken to ensure that the integrations are accurate (see below). All the available information about Γ is contained in the array of partial volumes.

Consider a cell centered at (ih, jh) crossed by Γ , i.e., $0 < f_{i,j} < 1$, as well as the eight adjacent cells. We shall be looking for a circle whose intersection with each of these nine squares has the same partial volumes as the ones that are given. This circle will be taken to be the osculating circle, its radius will be the radius of curvature, the inverse of its radius will be the curvature, and the radius vector leading to its center will be the normal to Γ .

Assume that, as in Fig. 1, the block of nine cells has been placed on the second quadrant of an auxiliary plane and write for short $f_{I,J} = f_{i+I-2, j+J-2}$, $I, J = 1, 2, 3$. First evaluate the corner sums $S_1 = f_{1,1} + f_{1,2} + f_{2,1} + f_{2,2}$, etc., and rotate the nine

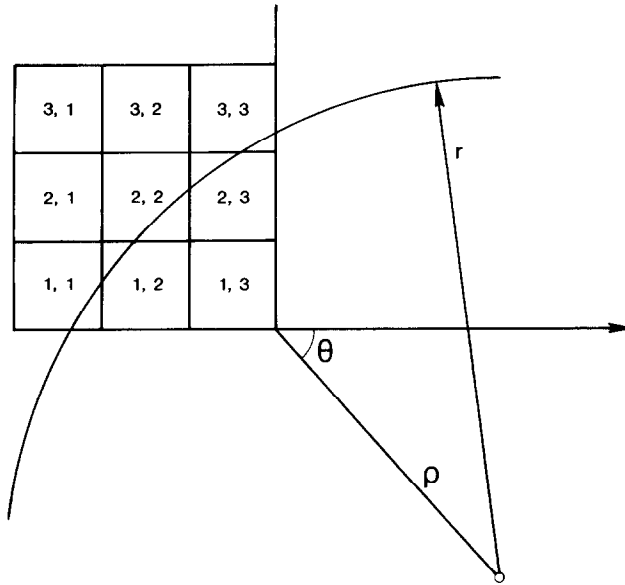


FIG. 1. The auxiliary plane for computing curvature.

cells if necessary so that the blackest corner is near the origin. If the radius of curvature r is positive, the center of curvature (i.e., the center of the osculating circle) is now in the fourth quadrant. Represent the center of curvature in polar coordinates as $(\rho \cos \theta, -\rho \sin \theta)$, $0 \leq \theta \leq \pi/2$.

Assume first that r is positive, and look for ρ , r , and θ by trial and error, i.e., assume values for these quantities, compute the corresponding partial volumes, and use these to improve the guess. The volume fractions are easier to evaluate if the arcs of the circle are nearer to the horizontal than to the vertical (Fig. 2), i.e., if $\theta \geq \pi/4$. One can readily see that $\pi/4 \leq \theta \leq \pi/2$ if $(f_{1,1} + f_{1,2} + f_{2,1}) \geq (f_{2,3} + f_{3,2} + f_{3,3})$. If this condition is not satisfied, the block of cells is reflected around the line joining $f_{1,3}$ and $f_{3,1}$. The partial volumes are computed by the trapezoidal rule, with m points of integration per square.

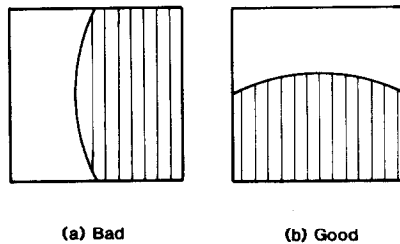


FIG. 2. Precautions in the computation of volume fractions.

Let ρ^n, θ^n, r^n be the tentative parameters describing the osculating circle; let $f_{i,j}^n$ be the corresponding partial volumes.

Define

$$\begin{aligned}
 C &= f_{2,2}, & C^n &= f_{2,2}^n, \\
 A &= \sum_{i,j} f_{i,j}, & A^n &= \sum_{i,j} f_{i,j}^n, \\
 \alpha &= \arctan \frac{f_{2,3} + f_{3,2} + f_{3,3}}{f_{1,1} + f_{1,2} + f_{2,1}}, \\
 \alpha^n &= \arctan \frac{f_{2,3}^n + f_{3,2}^n + f_{3,3}^n}{f_{1,1}^n + f_{1,2}^n + f_{2,1}^n},
 \end{aligned}$$

where the $f_{i,j}$ are the given partial volumes.

There are clearly many sets of values $f_{i,j}$ for which there exists no osculating circle; we assume first that the problem of finding ρ, θ, r does have a solution. If $C^n < C$ and $A^n < A$, the trial circle is too far and ρ should be decreased; if $C^n > C$ but $A^n < A$, the radius of the trial circle is too small, etc. After much trial and error we came up with an iteration scheme which converged in all the problems we tried; the iteration recognizes four cases:

Case I. $C^n < C, A^n < A$ (ρ should decrease). Define the following auxiliary quantities:

$$\begin{aligned}
 q_1 &= \min(C, 1 - C), \\
 q_2 &= \min(1, q_1), \\
 q_3 &= \max(q_2, \varepsilon), \\
 q_4 &= h/q_3, \\
 \beta_1 &= q_4 |C^n - C|,
 \end{aligned}$$

where ε is a small quantity (we usually took ε between 10^{-2} to 10^{-3}); if $\beta_1 \geq \varepsilon$, then set

$$b = \beta_1,$$

otherwise set

$$b = \max(\beta_1, \beta_2),$$

where

$$\beta_2 = h(\sin \theta) |A^n - A|/5,$$

and finally compute

$$\rho^{n+1} = \rho^n - b.$$

b is the appropriate decrease in ρ . The geometrical factors q_1, q_2, q_3, q_4 serve to modify b in cases where only a small piece of the middle square is either black or white and convergence could be very slow. β_2 is introduced to modify the change in ρ so as to avoid situations in which a circle that is too small is slowly moved towards the origin without an increase in its radius. A moment's thought will explain the geometrical factors $\sin \theta$ and 5.

Case II. $C^n > C, A^n > A$ (ρ should increase). b is defined as in Case I, and

$$\rho^{n+1} = \rho^n + b.$$

Case III. $C^n < C$ and $A^n > A$ (both ρ and r should increase). Define

$$b = \min((\rho^n)^2 |A^n - A|/2h, \rho^n/2),$$

and set

$$\rho^{n+1} = \rho^n + b + h(A^n - A),$$

$$r^{n+1} = r^n + b.$$

If $A^n < A$, one wishes $\rho^{n+1} - \rho^n$ to be as large as possible, but not so large that the correct ρ will be overshoot and oscillation will set in. The factor $(\rho^n)^2/2h$ and the restriction $b \leq \rho^n/2$ have been found to be satisfactory by trial and error.

Case IV. $C^n > C$ and $A^n < A$ (both ρ and r should decrease). b is defined as in Case III, and set

$$\rho^{n+1} = \rho^n - b + h(A^n - A),$$

$$r^{n+1} = r^n - b.$$

In all cases, we further compute

$$\theta^{n+1} = \theta^n + \frac{1}{2}(\alpha - \alpha^n),$$

and impose the restrictions

$$\frac{\pi}{4} \leq \theta^{n+1} \leq \frac{\pi}{2}, \quad \rho \geq h, r > 0.$$

If r becomes large, for example, $r > 100$ or $r > 1/\varepsilon$, one concludes that the assumption $r > 0$ is fallacious and one looks for an osculating circle centered on the other side of the curve. The same iteration can be used if the nine squares are reflected around the line connecting $(1, 1)$ with $(3, 3)$ and the $f_{i,j}$ are transformed into their complements $f'_{i,j} = 1 - f_{i,j}$. If r becomes large a second time, one concludes that the boundary is flat. The iteration is stopped when

$$|A^n - A| + |\theta^n - \theta| + |C^n - C| < \varepsilon.$$

If the nine numbers $f_{i,j}$ can be produced by the intersection of a circle with the nine cells, the iteration will exhibit that circle. It is possible to alter the “off diagonal” $f_{i,j}$ in such a way that the sums in the definition of the quantities θ, A, C are unchanged and a circle will still be produced, even though the $f_{i,j}$ individually can no longer be produced by that circle. One can experiment with various least squares and other fits in that case, but none seem to be practically superior or better justified than simply accepting the circle produced by the algorithm. Finally, there are many situations in which no circle can produce the given values of $\theta, A,$ and C ; the algorithm will then fail to converge. We decide that no convergence has taken place if the number of iteration exceeds some preset integer N (we usually used $N=35$, a value that is somewhat larger than necessary).

In many practical problems, the values of $\theta, r,$ and ρ at the end of the iteration at one point will serve as good starting values for the iteration at the next point.

A NUMERICAL EXAMPLE

There are many problems in which one can display a spectacular agreement between a known curvature and the curvature computed by the algorithm of the preceding section. In particular, the curvature of circles is reproduced with an accuracy that depends only on the number m of points in the quadrature formula and on the tolerance ϵ . With $m=15$ and $\epsilon=10^{-3}$ we get three good digits if the curvature is $O(1)$. It may be more instructive to consider a less well-behaved problem.

Consider the curve $y=1/2+(3/10)\sin 2\pi x$ for $0\leq x\leq 1$. Its curvature is $C(x)=\pm(12\pi^2/10)\sin(2\pi x)/(1+(9/25)\pi^2\cos^2(2\pi x))^{3/2}$. Place the curve on a 20×20 grid ($h=1/20$), evaluate the corresponding volume fractions, and then evaluate the curvature by our iteration. The partial volumes are defined in the squares $ih\leq x\leq(i+1)h, jh\leq y\leq(j+1)h$. There is more than one curvature per given value of i since two cells located above each other can be intersected by the curve. In Table I we exhibit the computed curvature and compare it with “exact” answers. The “exact answers” II is $C(x)$, the exact curvature, evaluated at the points $(i-1/2)h$, i.e., in the middle of the cells. The “exact answer” I is $C(x^*)$ evaluated at x^* defined by

$$\begin{aligned} x^* &= (i-1)h + f_{i,j}h && \text{if } f_{i-1,j} = 0, \\ &= (i-1)h + (1-f_{i,j})h && \text{if } f_{i-1,j} = 1. \end{aligned}$$

The point x^* is the location of the black/white interface according to a standard recipe for reconstructing a surface from partial volumes (see [13]). The numerical parameters are $m=15$ and $\epsilon=10^{-3}$, and an average of about 10 iterations per cell is needed for convergence. Note that the curvature changes by a large amount from

TABLE I

Computed vs. Exact Curvature for $y = \frac{1}{2} + \frac{3}{10} \sin 2\pi x$, $h = \frac{1}{20}$

| i | j | Computed curvature | Exact value I | Exact value II |
|-----|-----|-----------------------|-----------------------|-----------------------|
| 2 | 12 | 0.55 | 0.45 | 0.77 |
| 2 | 13 | 0.98 | 0.92 | 0.77 |
| 2 | 14 | 1.35 | 1.26 | 0.77 |
| 3 | 14 | 2.09 | 1.26 | 2.04 |
| 3 | 15 | 3.06 | 3.23 | 2.04 |
| 4 | 15 | 5.34 | 3.34 | 5.49 |
| 4 | 16 | 7.30 | 8.57 | 5.49 |
| 5 | 16 | 9.86 | 8.58 | 11.38 |
| 6 | 15 | 7.16 | 5.81 | 8.58 |
| 6 | 16 | 8.93 | 11.38 | 8.58 |
| 7 | 14 | 2.42 | 2.12 | 3.34 |
| 7 | 15 | 4.00 | 5.49 | 3.34 |
| 8 | 13 | 1.02 | 0.93 | 1.26 |
| 8 | 14 | 1.75 | 2.04 | 1.26 |
| 9 | 11 | 0.27 | 0.24 | 0.45 |
| 9 | 12 | 0.52 | 0.49 | 0.45 |
| 9 | 13 | 0.84 | 0.77 | 0.45 |
| 10 | 9 | -0.19 | -0.18 | 1.84×10^{-7} |
| 10 | 10 | 8.50×10^{-3} | 1.84×10^{-7} | 1.84×10^{-7} |
| 10 | 11 | 0.19 | 0.20 | 1.84×10^{-7} |
| 11 | 7 | -0.84 | -0.76 | -0.45 |
| 11 | 8 | -0.52 | -0.49 | -0.45 |
| 11 | 9 | -0.27 | -0.20 | -0.45 |
| 12 | 6 | -1.75 | -1.72 | -1.26 etc. |

point to point. The smoothness of the computed curvature function can be seen when one considers the arrangement of the points in the plane.

The agreement between the computed curvature and the exact curvature evaluated at x^* is better than the agreement between the two "exact" values of the curvature. Other choices of location for the interface also lead to different values for the "exact" curvature. The partial volumes do not determine the location of the interface accurately enough for the purpose of deciding where the analytical formula for the curvature should be evaluated, and the computed curvature is a better estimate of the curvature of the portion of the curve contained in a given cell than the analytical formula evaluated at an ill-determined point. Since points on the curve are hard to locate, second differences involving their locations are even more problematic, and attempts to evaluate the curvature in this case by the algorithms suggested in [12] or [20] lead to very large errors.

Note that the curvature is antisymmetric around $x = \frac{1}{2}$; we display a few values for x larger than $\frac{1}{2}$ in order to show that the algorithm makes the right decisions about the sign of the curvature without outside prompting.

AN ENTHALPY FORMULATION OF THE STEFAN PROBLEM

Before considering the problem of unstable solidification, in which curvature plays an important role and to which we shall apply the algorithm of the preceding section, we discuss the easier, curvature-independent, Stefan problem. A collection of recent papers on the subject can be found in [23]. We restrict our attention to the enthalpy formulation because it will allow us in the next section to formulate an appropriate curvature/phase iteration. We begin with the case of a single space dimension.

The x axis is divided into disjoint sets I, W ; I is filled with a solid called "ice" and W is filled with "water." A temperature field is given at $t = 0$. At points interior to either I or W the evolution of the temperature is described by the heat equation; for the sake of simplicity we assume the thermal diffusivities of both "ice" and "water" are equal to 1 (the case of phases with non-equal diffusivities can be readily handled by the method of alternate phase truncation [14]). In $I, T = T_I \leq 0$; in $W, T = T_W \geq 0$. The latent heat of change of phase is $H > 0$. At the boundary between I and W we require that

$$T = 0, \tag{1a}$$

$$-\frac{\partial T_W}{\partial x} + \frac{\partial T_I}{\partial x} = HV, \tag{1b}$$

where V is the velocity of the ice/water interface, counted as positive if water is freezing. For the sake of simplicity, it is assumed that the heat capacity of both water and ice is 1. Equation (1b) expresses the conservation of energy at the interface.

Define the enthalpy u by

$$\begin{aligned} u &= T && \text{for } T \leq 0, \\ &= T + H && \text{for } T > 0. \end{aligned}$$

T can be expressed in terms of u by

$$\begin{aligned} T(u) &= u && \text{for } u \leq 0, \\ &= u - H && \text{for } u \geq H, \\ &= 0 && \text{for } 0 < u < H. \end{aligned}$$

The solution of the problem is the weak solution of the equation

$$u_t = T(u)_{xx}, \tag{2}$$

where t is the time and the subscripts denote differentiations. Equation (2) can be solved numerically. Existence, convergence, and uniqueness theorems can be found

in [1, 8, 14]; it follows from [14] that if Eq. (2) is discretized in time and space, then under broad conditions the leading term in the error is $O(k \log(t/k))^{1/2}$, where k is the time step.

Pick the simplest approximation to Eq. (2): write $u_i^n \equiv u(ih, nk)$, $T_i^n = T(u_i^n)$, and let

$$u_i^{n+1} - u_i^n = \frac{k}{h^2} (T_{i+1}^n + T_{i-1}^n - 2T_i^n). \tag{3}$$

This scheme converges for $k/h^2 \leq 1/2$. The following heuristic argument explains why the scheme converges.

In both I and W , Eq. (2) reduces to a standard heat equation, for which the scheme (3) is a reasonable approximation. Assume that for $i < i_0$ we have ice, for $i > i_0$ we have water, and at i_0 we have $0 < u_i^n < H$, i.e., the phase is undefined and we have ‘‘mush.’’ At i_0 Eq. (3) reduces to

$$u_{i_0}^{n+1} - u_{i_0}^n = k \left[\frac{T_{i_0+1}^n - 0}{h} - \frac{T_{i_0}^n - 0}{h} \right] / h. \tag{4}$$

$(T_{i_0+1}^n - 0)/h$ is an approximation to $\partial_x T_W$, if we assume that the interface is at $x_0 = i_0 h$. Similarly, $(0 - T_{i_0}^n)/h$ is an approximation to $\partial_x T_I$. The value of u is changing at a rate approximately proportional to $(\partial_x T_W - \partial_x T_I)/h$. Suppose the area occupied by water is expanding. During the time $i_0 h$ is a mush point u_{i_0} changes from 0 to H ; thus the front moves a distance h during the time it takes u_{i_0} to grow from 0 to H at the rate $(\partial_x T_W - \partial_x T_I)/h$ and Eq. (1b) is satisfied on the average. Of course, the freezing point is not located exactly at $i_0 h$ during all this time and thus the balance equation (4) is correct only in an average sense. Most importantly, one also concludes that u_{i_0}/H is the approximate partial volume of water in the cell $(i_0 - \frac{1}{2})h \leq x \leq (i_0 + \frac{1}{2})h$.

One can use the last remark to construct a better approximation to the solution of the Stefan problem. It is easy to see (see Table II below) that error is generated mainly at the interface. One can try to locate the interface accurately with the help of the computed partial volumes, and then apply condition (1b) accurately in the neighborhood of that interface. A construction in that spirit was given by Smith [20] in the two-dimensional case. Our experience has been that such constructions increase the accuracy at the beginning of the calculation, but that the increased accuracy does not survive for long; we omit the details of the construction.

In Table II we exhibit the results of a calculation with a one-dimensional test problem. The region of integration is $0 \leq x \leq 1$; H is equal to 1. The initial conditions are

$$\begin{aligned} u(x, 0) &= \exp(0.5 - x) - 1 && \text{for } x > 0.5, \\ &= 2 \exp(0.5 - x) - 1 && \text{for } x < 0.5. \end{aligned}$$

TABLE II
Errors in One-Dimensional Model Stefan Problem

| | Straightforward enthalpy formulation | Modified formulation |
|---|---|-----------------------|
| (1) after one step ($t = 6.17 \cdot 10^{-3}$) | | |
| | $-3.95 \cdot 10^{-5}$ | $-3.95 \cdot 10^{-5}$ |
| | $-3.56 \cdot 10^{-5}$ | $-3.56 \cdot 10^{-5}$ |
| | $-3.17 \cdot 10^{-5}$ | $-3.17 \cdot 10^{-5}$ |
| | $-1.02 \cdot 10^{-5}$ | $-8.69 \cdot 10^{-5}$ |
| | — | — |
| | $-5.11 \cdot 10^{-4}$ | $-4.10 \cdot 10^{-5}$ |
| | $-1.02 \cdot 10^{-5}$ | $-1.02 \cdot 10^{-5}$ |
| | $-9.11 \cdot 10^{-6}$ | $-9.11 \cdot 10^{-6}$ |
| (2) after 10 steps ($t = 6.17 \cdot 10^{-2}$) | | |
| | $-8.29 \cdot 10^{-3}$ | $3.60 \cdot 10^{-4}$ |
| | $-2.06 \cdot 10^{-2}$ | $8.89 \cdot 10^{-4}$ |
| | $-4.12 \cdot 10^{-2}$ | $1.51 \cdot 10^{-3}$ |
| | $-7.55 \cdot 10^{-2}$ | $2.08 \cdot 10^{-3}$ |
| | — | — |
| | $-3.75 \cdot 10^{-2}$ | $1.56 \cdot 10^{-3}$ |
| | $-1.98 \cdot 10^{-2}$ | $1.08 \cdot 10^{-3}$ |
| | $-8.43 \cdot 10^{-3}$ | $5.74 \cdot 10^{-4}$ |
| (3) after 40 steps ($t = 0.247$) | | |
| | $-3.95 \cdot 10^{-3}$ | $-1.52 \cdot 10^{-3}$ |
| | $-7.32 \cdot 10^{-3}$ | $-3.59 \cdot 10^{-3}$ |
| | $-7.73 \cdot 10^{-3}$ | $-8.57 \cdot 10^{-3}$ |
| | $-9.25 \cdot 10^{-3}$ | $-1.00 \cdot 10^{-2}$ |
| | $-1.18 \cdot 10^{-2}$ | $-1.67 \cdot 10^{-2}$ |
| | $-2.42 \cdot 10^{-2}$ | $-1.51 \cdot 10^{-2}$ |
| | — | — |
| | $-9.86 \cdot 10^{-3}$ | $-3.90 \cdot 10^{-3}$ |

The boundary conditions are

$$u(0, t) = \exp(t + 0.5) - 1,$$

$$u(1, t) = 2 \exp(t - 0.5) - 1,$$

The solution of the problem is

$$u(x, t) = \exp(t - x + 0.5) - 1 \quad \text{for } t - x > 0.5,$$

$$= 2 \exp(t - x + 0.5) - 1 \quad \text{for } t - x < 0.5.$$

The water/ice interface starts at $x = 0.5$ and moves with velocity one in the direction of increasing x . The numerical parameters are $h = \frac{1}{5}$, $k/h^2 = 0.5$.

In Table II we display the errors in the solution of this problem, i.e., the differences between the computed and the exact solution, for $x = ih$, $i = 1, \dots, 8$. At the point where $0 < u < H$, i.e., boundary point between ice and water, there is no reasonable definition of the error. As one can see from the table, the error radiates from the discontinuity; the more "accurate" method has a decided advantage over the straightforward solution for the first 10–20 steps, but by step 40 the two are comparable. We have no analysis of this phenomenon, except for the observation that similar phenomena have been observed in the case of hyperbolic equations with discontinuous solutions (see [4, 9, 11]). Higher accuracy can be recovered in linear hyperbolic problems if appropriate processing is applied to the data and/or the solution; if such processing exists for the Stefan problem, we have not been able to find it. The variation of the error as a function of k and h agrees with the results in [14] and will not be displayed.

The enthalpy method generalizes to multi-dimensional problems. In two space dimensions Eq. (2) becomes

$$u_t = \Delta T(u), \quad \Delta = \text{Laplace operator.} \tag{5}$$

The boundary conditions at the water/ice interface become

$$T = 0, \tag{6a}$$

$$-\frac{\partial T_w}{\partial n} + \frac{\partial T_I}{\partial n} = HV_n, \tag{6b}$$

where $\partial/\partial n$ denotes differentiation in the direction normal to the interface, and V_n is

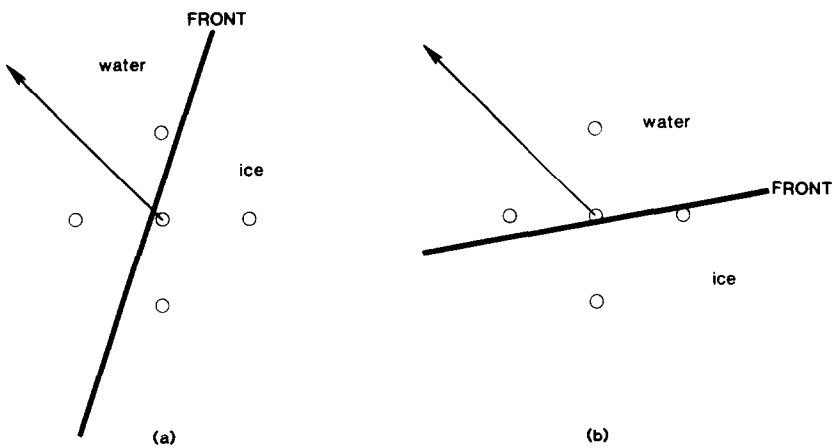


FIG. 3. Origin of grid effects with a five-point Laplacian.

the normal velocity of the interface. On the border of $I \cup W$ a boundary condition on u or T is also needed.

The difference approximation (3) can be readily generalized to the case of two dimensions; analysis and examples can be found in [1, 14]. The error $O(k \log(t/k))^{1/2}$ will restrict us to small time steps, and we see no reason to abandon explicit schemes.

It is important to point out that the boundary condition (6b) will be satisfied only on the average in space as well as on the average in time. This is due to grid effects, which can be best understood by example. Consider a front separating ice and water, and suppose ΔT is computed by the usual five-point formula (Fig. 3). It is easy to see that in both cases (a) and (b) of Fig. 3, in which the directions of the fronts are quite different from each other, the effective normal to the interface in the evaluation of the boundary condition (6b) is the same. This grid effect can be reduced by constructing approximations to the Laplacian which have as much rotation invariance as possible. A construction suggested by the Huygens principle of [2] is

$$\begin{aligned}
 h^2 \tilde{\Delta}_h T = & \frac{1}{1 + \beta} (T_{i,j+1} + T_{i,j-1} + T_{i+1,j} + T_{i-1,j} - 4T_{i,j}) \\
 & + \frac{\beta}{2(1 + \beta)} (T_{i+1,j+1} + T_{i-1,j-1} + T_{i+1,j-1} + T_{i-1,j+1} - 4T_{i,j}). \quad (7)
 \end{aligned}$$

Numerical experiment suggests that the value $\beta = 1/\sqrt{2}$ is best. Equation (5) can now be approximated by

$$u^{n+1} = u^n + k \tilde{\Delta}_h T(u).$$

This scheme is stable if

$$\frac{k}{h^2} \leq \frac{1}{4} \frac{\beta + 1}{1 + \beta/2}.$$

In the problem discussed in the present section, the difference between the solution obtained with the usual five-point approximation and the one obtained with $\tilde{\Delta}_h$ is not significant.

UNSTABLE SOLIDIFICATION

A relatively simple model problem involving unstable solidification and possible dendrite formation is discussed in Langer [7], Sekerka [15], and Smith [20]. It involves two phases, "ice" and "supercooled water," i.e., water that has been

allowed to cool below zero without freezing. At the interface between ice and water, the following conditions are imposed:

$$T = -\kappa C, \quad (8a)$$

$$-\frac{\partial T_w}{\partial n} + \frac{\partial T_I}{\partial n} = HV_n. \quad (8b)$$

Equation (8b) is identical to Eq. (6b), with T_w denoting the temperature of supercooled water. Equation (8a) is a form of the Gibbs–Thomson relation (see, e.g., [21]); κ is a constant and C denotes the curvature of the interface, taken as a positive if the circle of curvature lies on the ice side of the interface.

The enthalpy formulation of the preceding section can be adapted to this problem. Equation (5) survives: $u_t = \Delta T(u)$. However, the relation between T and u must be re-examined. It is clear from physical considerations and from the requirement that our problem have a unique solution that supercooled water can be allowed to freeze only where it is adjacent to ice, and conversely ice can be allowed to melt only when it touches water (see Smith [20]). Suppose at $t=0$ we have a region I occupied by ice, a region W occupied by water, and a region M of mathematical mush between I and W ; M is made up of cells which are crossed by the water/ice interface. In I , $T = u$; in W , $T = u - H$ even if $T \leq 0$; in M , $T(u)$ must be chosen so that condition (8a) is satisfied; condition (8b) will be satisfied if conservation of energy is enforced. T is assumed given at the boundary of $T \cup W$. The first problem is to determine which cells belong to M .

Each cell has eight neighbors, all of which participate in the difference operator (7). M is a subset of those cells which do not contain ice but have a neighbor containing ice. However, not all the cells which are neighbors of I necessarily belong to M . It is easy to see that just as in the case of ordinary, non-supercooled water, the calculation can occasionally produce a cell of water and a cell of ice lying next to each other. A reasonable test for deciding whether a mesh cell (i, j) abutting on ice contains water or mush is the following: Consider those neighbors of (i, j) that are known to contain water as well as their neighbors, and determine by linear interpolation a reasonable water temperature $\tilde{T}_{i,j}$ in (i, j) . If $u_{i,j} - H < \tilde{T}_{i,j}$, (i, j) is filled with mush, and if $u_{i,j} - H \geq \tilde{T}_{i,j}$, (i, j) is filled with water. Having determined M , the mush region, one can determine the curvature C of the interface and then set $T = -\kappa C$ in M .

The determination of C involves an iteration (similar in principle, but not in detail, to the iteration described in [20]). Indeed, the curvature C depends on the array of volume fractions of ice in the cells of M , but these volume fractions depend on the temperature of change of phase and therefore on C . The natural iteration proceeds as follows: One starts with a guess for the array of C 's (an appropriate guess is always available from the previous step or from the initial conditions). Suppose u in a cell believed to be in M satisfies $u \geq -\kappa C + H$, then the cell really belongs to W and is removed from M . Suppose $u \leq -\kappa C$, then the cell belongs to I . If neither of these conditions holds, then the ice volume fraction in the cell is

$1 - (u + \kappa C)/H$. One now finds new C 's by the curvature algorithm described above. For convergence, one must underrelax, i.e., the new curvature at a point at the end of an iteration is set equal to the average of the newly computed curvature and of the curvature available at end of the previous iteration. The relative ease with which this iteration can be set up within the framework of the enthalpy formulation is that formulation's main attraction. However, the iteration converges slowly; as many as 30 iterations may be needed with a reasonable criterion for convergence and the expense is considerable. The reason for the slow convergence is likely to be the ill-conditioned nature of the phase/curvature relation. A small change in the shape of the ice region can produce a large change in curvature and thus a substantial change in the temperature of phase transition. It is rather surprising that the iteration converges at all except when all the perturbations are small. One should note that the finite cell size imposes a bound on the possible perturbations in curvature, and one may well wonder if the problem does remain well posed when the cell size shrinks to zero. In fact, one may wonder whether linear perturbation theory applies to the solidification problem in a supersaturated medium unless one can somehow restrict oneself to smooth perturbations (for further comments, see below).

Having found the curvature C , one has $T(u)$ everywhere and one can use a difference scheme to advance the enthalpy. The scheme (7) is both experimentally and theoretically preferable to a scheme with a smaller stencil and will be used throughout the calculations of the present section. Having determined u , new domains I , W , and M can be determined, new values of C can be found, etc.

Some precautions must be observed:

(i) As stated above, water can freeze and ice can melt only after a passage through a state of mush.

(ii) T is typically at a maximum in M , since both ice and supercooled water can be colder than zero. If, in the application of the difference scheme, we allow W and I to be neighbors, the maximum will be smeared and the region of mush will spread uncontrollably. On the other hand, the mush region M as determined above may fail to separate I and W , and thus additional, artificial, and temporary mush cells must occasionally be created. To avoid a systematic bias, we create them alternately on the water side and on the ice side of the water/ice interface. An appropriate curvature at these extra mush points is found by averaging the curvature at the neighboring points of the mush region M .

(iii) The variation of the values of u at the cells of M clocks the passage of the interface through these cells. The first time a cell joins M the "clock" may fail to be at zero since the values of u and C depend on the history of the cell and of its neighbors and on the gradients of T in the region of supercooled water. An adjustment must be made to the value of u at a newly identified cell in M , and that cell must then be exempted from tests that may reassign it immediately back to I or W .

(iv) The curvature algorithm may fail to converge. If that happens, it is preferable to use an old value of C or an average of neighboring values of C rather than rely on a possibly meaningless number.

We try our method on the first test problem of Smith [20]. At $t=0$ a cylinder of ice of radius $R_0=0.15$ is surrounded by supercooled water. At $r=\sqrt{x^2+y^2}=0.5$ we impose the boundary condition $T=-1$, and set $H=2$. In the quasi-stationary approximation (in which it is assumed that the front moves slowly compared to the speed with which the heat distribution relaxes to equilibrium (see [7, 15])), there is a solution satisfying these conditions:

$$\begin{aligned} T(r) &= -\kappa/R + \alpha \log(r/R), & r \geq R, \\ &= -\kappa/R, & r < R, \end{aligned}$$

where $\alpha = (1 - \kappa/R)/\log(2R)$, and R is the radius of the growing cylinder of ice. The growth velocity is

$$\dot{R} = \frac{dR}{dt} = \frac{(1 - \kappa/R)}{HR \log(1/2R)}. \quad (9)$$

We impose initial conditions on T compatible with this solution. The stability of this solution is discussed in [7, 15]. We pick $\kappa=0.01$; the interface should then be stable. In Table III we exhibit the computed $R = \sqrt{A/\pi}$, where A = the area of ice, the computed growth velocity $\dot{R} = (R(t+k) - R(t))/k$, where k is the time step, the average computed \dot{R} , averaged from $t=0$ to the current time, and the value of \dot{R} given by the quasi-stationary approximation, with $h=1/35$ and k at the limit of numerical stability, $k=2.88 \times 10^{-4}$. For the times exhibited, the agreement is excellent, and it remains excellent for a long time; when $R=20$, the average computed \dot{R} is 2.55 while the quasi-stationary \dot{R} given by formula (9) is 2.59. The two-step oscillation in \dot{R} observed from time to time is due to the alternation in the location of the temporary mush cells described under precaution (ii) above, and has no particular significance. It is natural to compare the analytical solution with an average solution, for the reasons described in the preceding section.

The agreement is, however, not perfect in other respects. The shape of the ice region remains as perfectly circular as can be decided on the basis of the available partial volumes until $R \sim 0.18$, but then it begins to oscillate slightly. The curvature C is never perfectly constant. In Table IV we exhibit some values of C at $R \sim 0.18$, drawn from a calculation with $h=1/20$. There is a bulge at the four corners corresponding to the lines $y = \pm x$. This bulge will eventually be damped, and, after $R \sim 0.18$, the shape of the frozen area will oscillate, and the distance between the center of the ice and a point on the interface will eventually vary by as much as 10%. This phenomenon is roughly independent of h in our experiments, $1/20 \leq h \leq 1/60$. These observations are apparently in agreement with the observations of Smith, and are surprising because according to linear stability theory we

TABLE III
Solution of Solidification Problem

| R | Computed \dot{R} | Averaged computed \dot{R} | Quasi-stationary \dot{R} |
|---------|--------------------|-----------------------------|----------------------------|
| 0.14999 | 0.000 | 0.000 | 2.584 |
| 0.15075 | 2.611 | 2.611 | 2.582 |
| 0.15150 | 2.614 | 2.612 | 2.581 |
| 0.15228 | 2.700 | 2.642 | 2.580 |
| 0.15308 | 2.770 | 2.674 | 2.579 |
| 0.15389 | 2.801 | 2.699 | 2.578 |
| 0.15470 | 2.824 | 2.720 | 2.576 |
| 0.15552 | 2.841 | 2.737 | 2.575 |
| 0.15634 | 2.841 | 2.750 | 2.574 |
| 0.15716 | 2.817 | 2.758 | 2.574 |
| 0.15796 | 2.794 | 2.761 | 2.573 |
| 0.15876 | 2.750 | 2.760 | 2.572 |
| 0.15950 | 2.557 | 2.743 | 2.571 |
| 0.16005 | 1.933 | 2.681 | 2.571 |
| 0.16101 | 3.319 | 2.727 | 2.570 |
| 0.16131 | 1.030 | 2.613 | 2.570 |
| 0.16223 | 3.184 | 2.649 | 2.569 |
| 0.16244 | .733 | 2.536 | 2.569 |
| 0.16335 | 3.161 | 2.571 | 2.568 |
| 0.16476 | 2.865 | 2.557 | 2.567 |
| 0.16550 | 2.582 | 2.558 | 2.567 |
| 0.16643 | 3.229 | 2.589 | 2.566 |
| 0.16717 | 2.548 | 2.587 | 2.566 |
| 0.16798 | 2.814 | 2.596 | 2.566 |
| 0.16879 | 2.792 | 2.604 | 2.566 |
| 0.16982 | 3.573 | 2.641 | 2.565 |
| 0.17052 | 2.438 | 2.634 | 2.565 |
| 0.17122 | 2.425 | 2.626 | 2.565 |
| 0.17199 | 2.649 | 2.627 | 2.565 |
| 0.17260 | 2.127 | 2.611 | 2.565 |
| 0.17331 | 2.445 | 2.605 | 2.565 |
| 0.17392 | 2.120 | 2.590 | 2.565 |
| 0.17442 | 1.735 | 2.564 | 2.565 |
| 0.17525 | 2.869 | 2.573 | 2.566 |
| 0.17590 | 2.528 | 2.564 | 2.566 |
| 0.17670 | 2.760 | 2.570 | 2.566 |
| 0.17736 | 2.279 | 2.562 | 2.566 |
| 0.17820 | 2.937 | 2.572 | 2.567 |
| 0.17892 | 2.478 | 2.569 | 2.567 |

TABLE IV
 Computed Curvatures in the
 Growing Circular Icicle Problem

| <i>i</i> | <i>j</i> | Computed curvature (exact value: 5.89) |
|----------|----------|---|
| 8 | 8 | 7.57 |
| 8 | 9 | 7.58 |
| 8 | 10 | 4.71 |
| 8 | 11 | 4.53 |
| 8 | 12 | 4.71 |
| 8 | 13 | 7.58 |
| 8 | 14 | 7.57 |
| 9 | 8 | 7.58 |
| 9 | 14 | 7.58 |
| 10 | 8 | 4.71 |
| 10 | 14 | 4.71 |
| 11 | 8 | 4.53 |
| 11 | 14 | 4.53 |
| 12 | 8 | 4.71 |
| 12 | 14 | 4.71 |
| 13 | 8 | 7.58 |
| 13 | 14 | 7.58 |
| 14 | 8 | 7.57 |
| 14 | 9 | 7.58 |
| 14 | 10 | 4.71 |
| 14 | 11 | 4.53 |
| 14 | 12 | 4.71 |
| 14 | 13 | 7.58 |
| 14 | 14 | 7.57 |

are in a stable regime. The validity of the quasi-stationary approximation can be checked on the computer and is not in question with our parameter values.

The oscillation can be partially ascribed to numerical error. The curvature is dependent on second derivatives of the functions that describe the interface, and cannot be accurate if that interface is not computed accurately. Here one should emphasize the significance of the "grid effects" mentioned earlier. Suppose one solves a differential equation and obtains a numerical solution that is accurate to some order. If the error has an asymptotic error expansion, then the computed solution can be differenced and yields approximations to the derivatives of the solution of the same order of accuracy as the approximation of the solution itself. In the presence of "grid effects" the functions that describe the interface do not have an asymptotic error expansion, and the curvature algorithm, accurate though it may be, is at least partly stymied by the inadequacy of the data on which it operates.

This is not, however, a fully satisfactory explanation. One would expect that small, numerically induced perturbations on a stable surface would be damped

quickly, and this does not happen; the bumps in the surface, though they do not grow catastrophically, oscillate and do not decay as the linear theory predicts. A possible explanation is that, as in other front stability problems, the linearized theory does not predict correctly the response of the system to a perturbation of finite amplitude. For example, Landau instability of flames does not occur because flame fronts develop cusps (see Sethian [16, 18]). Fronts in porous media respond to perturbations as per the predictions of the linear theory only when the perturbations are extremely small (see [3]). The ill-conditioned nature of the phase/curvature relation, discussed above, casts a further doubt on the validity of a linearized stability theory in which it is assumed the perturbations are smooth. Thus, the numerical errors in the shape of the surface may be interacting with a underlying physical finite amplitude instability to create a morphological oscillation. If such a finite amplitude instability does indeed exist, and is related to the ill-conditioned nature of the phase/curvature relation, then it is questionable whether Eqs. (2) and (8) provide a reasonable mathematical model of the physical situation they are meant to describe.

Note. The programs used above can be obtained from the author.

ACKNOWLEDGMENTS

I would like to thank Chris Anderson, Richard Ghez, Ole Hald, Andrew Majda, and James Sethian for very helpful discussions.

REFERENCES

1. H. BREZIS AND M. CRANDALL, *J. Math. Pures Appl.* **58** (1979), 153.
2. A. J. CHORIN, *J. Comput. Phys.* **35** (1980), 1.
3. A. J. CHORIN, *Commun. Math. Phys.* **91** (1983), 103.
4. B. ENGQUIST, private communication (1981).
5. A. F. GHONIEM, A. J. CHORIN, AND A. K. OPPENHEIM, *Philos. Trans. R. Soc. London Ser. A* **304** (1982), 303.
6. C. W. HIRT AND B. D. NICHOLS, *J. Comput. Phys.* **39** (1981), 201.
7. J. S. LANGER, *Rev. Mod. Phys.* **52** (1980).
8. A. MAJDA, Lectures on partial differential equations, University of California, Berkeley, Mathematics Department (1982).
9. A. MAJDA AND S. OSHER, *Commun. Pure Appl. Math.* **30** (1977), 671.
10. G. H. MARKSTEIN, "Unsteady Flame Propagation," Pergamon, New York, 1966.
11. M. MOCK AND P. D. LAX, *Commun. Pure Appl. Math.* **31** (1978), 423.
12. B. D. NICHOLS, C. W. HIRT, AND R. S. HOTCHKISS, Report LA-8355, Los Alamos Scientific Lab. (1980).
13. W. NOH AND P. WOODWARD, in "Proceedings, 5th Int. Conf. Num. Methods Fluid Dynamics" (A. I. Van de Vooren and P. J. Zandbergen, Eds.), Springer Pub., New York, 1976.
14. J. C. W. ROGERS, A. E. BERGER, AND M. CIMENT, *SIAM. J. Numer. Anal.* **16** (1979), 563.
15. R. F. SEKERKA, Morphological stability, in "Crystal Growth, an Introduction" (P. Hartman, Ed.), North-Holland, New York, 1973.

16. J. SETHIAN, Ph. D. thesis, Mathematics Department, University of California, Berkeley (1982).
17. J. SETHIAN, *J. Comput. Phys.* **54** (1984), 425–456.
18. J. SETHIAN, Fronts, cusps, and curvature, in preparation.
19. N. SHAMSUNDAR AND E. M. SPARROW, *J. Heat Transfer* **20** (1975), 333.
20. J. SMITH, *J. Comput. Phys.* **39** (1981), 112.
21. J. J. STOKER, “Water Waves,” Interscience, New York, 1957.
22. D. TURNBULL, Phase changes, in “Solid State Physics” (F. Seitz and D. Turnbull, Eds.), Academic, New York, 1956.
23. D. A. WILSON, A. D. SOLOMON, AND P. T. BOGGS, “Moving Boundary Problems,” Academic, New York, 1978.